Journal of Engineering Physics and Thermophysics, Vol. 75, No. 3, 2002

REVIEW

MODERN NOTIONS OF THE EFFECT OF SUPERDEEP PENETRATION

S. M. Usherenko

UDC 534.2

This paper considers a number of questions of mass transfer and energy redistribution in a nonstationary process – superdeep penetration (SDP) of a flux of microstrikers into metal obstacles. On the basis of the set of known results, under the assumption of a dynamic phase transition inhibited at the stage of loss of long links due to the severe deformation an approach to the understanding of this phenomenon is proposed and estimates of the energetics of the SDP process are made.

Introduction. In the process of the development of technical civilization, questions of collisional interaction have been given much consideration.

By the middle of the last century, it had been established that practically under any striking conditions the crater depth cannot exceed 10 gauges of the striker. Thus, not quite deliberately the physical barrier to penetration at a collision was determined. The numerous investigations on the piercing of obstacles carried out in different countries permit solving problems on increasing the cratering depth within these limits. Typical of the current level of technical development is the fact that the experimental results falling outside this barrier are called anomalous and do not attract particular attention.

In 1974, we performed for the first time an analysis of the anomalies in the crater formation, which showed that the so-called anomalous results were obtained in the region of interaction with microobjects. The first experimental condition for reproducing the collisional penetration was formulated. Craters with a ratio of the depth to the striker size above 10 are registered in bombarding the obstacle by a flux of strikers measuring less than 500 μm [2].

By 1987, the experimental results on superdeep penetration were universally recognized and a lengthy discussion about its mechanism was stirred up. Already at the first stage of the search for explanations of the sudden drop of resistance to the introduction of the striker, notions of the meltdown of the channel-crater volume were rejected. As a physical approach to the explanation of this effect, notions of the retardation of the elastic state phase in the process of loading with a flux of microstrikers and of the formation of mode I cracks [3] were used. Such an approach made it possible to obviate the question of shortage of energy for cratering. However, the SDP evaluation in terms of the crack extension encounters limitations associated with the presence in the channel zone of intensive plasticity and thermal effects. Subsequently, a model assuming the presence of a crack in the form of a cylinder had to be developed. But as a result of a continuous series of assumptions, this approach proved to be ineffective.

The theory developed by P. B. Makarov and J. S. Doronin deserves separate consideration. They proposed a model based on the cumulation of micropores and extended microcraters with vortex formation. The pressure in the microcumulation zone is estimated to be up to 100 GPa and the background pressure is of the order of 2 GPa [4].

However, such notions did not receive further development and are not considered in the present work.

Analysis of the Penetration Process. The collisional interaction of bodies has been a traditional dynamical problem throughout all time. Accumulation of information on practical and model solutions of this problem has been going on for millenia. In the middle of the 20th century, the analysis of the obtained data revealed the presence of a barrier limitation in the piercing process. The increase in the collision energy and the change in the collision angle and densities of interacting bodies made it impossible to obtain a ratio between the piercing (crater) depth and the deter-

Scientific-Research Institute of Pulsed Processes of the Belarusian State Scientific-Production Powder Metallurgy Concern. Translated from Inzhenerno-Fizicheskii Zhurnal, Vol. 75, No. 3, pp. 183–198, May–June, 2002. Original article submitted June 29, 2201; revision submitted August 19, 2001.

1062-0125/02/7503-0753$27.00

mining geometrical parameter of the striker above 10. It was established that the energy introduced at a collision of individual macro- and microstrikers is mainly expended in mass ejection, melting, and emission rather than in increasing the relative penetration depth.

In considering the questions of piercing, it was noted that the strength of the obstacle material is significant in the range of pressures slightly below 100 kbars, and for the majority of materials its influence is significant at pressures in the collision zone below 10 kbars [5].

The review of the information on the formation of crater structures revealed the general laws of cratering and specific differences [6]. Consideration was given to the values of the expansion velocity of a substance at an impact. One differentiates between the "early" period of ejection accompanied by the appearance of a reverse cumulative jet and "late" ejection. The second stage of ejection is characterized by a low ejection velocity of the material from the crater and is realized, as is believed, at the hydrodynamic stage of the funnel growth. According to [7], no more than 5% of the ejected mass has a velocity above 1000 m/sec. In bombarding a gold target by iron microparticles at a velocity of 4810 m/sec, the initial ejection displayed a velocity of up to $3 \cdot 10^4$ m/sec, and the second ejection (up to 90% of the ejected mass) occurred at a velocity of up to $2 \cdot 10^3$ m/sec [8]. It was shown that when steel balls stroke against an iron obstacle, the initial ejection had a velocity above $3 \cdot 10^3$ m/sec, and the mass thrown in this period constituted $7.5 \cdot 10^{-5}$ of the mass of the striker, i.e., less than a hundredth of a percent [6]. Results on the striking of iron microparticles weighing 10^{-11} g at a velocity of up to $6 \cdot 10^3$ m/sec against glass were presented. A mass ejection of $18 \cdot 10^{-11}$ g at a velocity less than $5 \cdot 10^2$ m/sec was established. A case where 40 masses of the striker were ejected at a velocity of $24 \cdot 10^3$ m/sec under interaction of a bunch of tungsten particles was reported.

Original investigations on the striking with a velocity of $7 \cdot 10^3$ m/sec against sand were carried out [9]. The method of coloring different layers of sand was used. This experiment makes it possible to consider the interaction with an obstacle whose material has no strength. It was established that only a small portion of the crater volume is formed by the ejection. Its major portion is formed due to the displacement of the obstacle material to the sides and downward. By virtue of the experimental assumptions made, this variant of collisional interaction is not typical of the striking of a macrobody against an obstacle.

The universally accepted approach in analyzing the cratering is determination of the dependence of crater sizes on the volume energy density and the strength properties of the obstacle material [10]. It is customary to assume that typical crater formations are hemispherical, lens-shaped cavities with a flat portion of the bottom. Bell-shaped craters [11, 12] are characterized by specialists as nontypical.

The results on the formation of flask-shaped craters with a relative depth of more than 10 gauges are assumed to be anomalous [13]. They were registered for the case of interaction of a bunch of tungsten and zirconium particles of an 80–100 μm fraction with an iron obstacle.

Analysis of the typical crater structures permits analogy with a vessel having an open upper part. Because of the considerable statistical and dynamic resistances, the displacement of the crater walls and bottom is inhibited (the stress at these boundaries should exceed the dynamic yield stress). Therefore, the major portion of energy is carried away through the free surface of the vessel. Heat losses through the crater walls and bottom are small, because the collisional interaction time is less than 10 μsec, as a rule, and the heat-conductivity coefficient is actually a constant depending on the obstacle material. Under the conditions of an open system, the energy capacity of the obstacle material can also be considered to be a constant. The volume of a typical crater is no less than four volumes of the striker. Since it is customary to assume that the primary ejection is a result of the cumulative jet formation, it is created only in the case where the stage of crater collapse is significant. Proceeding from this statement, we can explain the spread of values for the primary ejection.

It is customary to consider four stages of cratering. At the first stage, the pressure on the walls exceeds the dynamic yield stress and the crater volume grows fast until it reaches the size of the striker or its implanted part. The second stage is realized due to the fact that the layer of the deformed material of the walls has the residual velocity acquired at the first stage. This can be superimposed by the dynamic pressure arising from the striker destruction and the pressure of its components on the walls. It is obvious that the load of the striker residue on the walls due to the flow onto the open surface will be much greater than the analogous action on the bottom of the vessel. The third stage is realized at the moment when the pressure on the walls and the bottom of the vessel turns out to be lower than the dynamic yield stress. Owing to the elastic component of the stress of the obstacle material compression of the

walls and a rise of the bottom of the vessel will take place to decrease the crater volume. Since, by virtue of the conditions of the second stage, the wall deformation turns out to be more significant than the deformation of the vessel bottom and the defective material layer, accordingly, thicker, the crater volume decreases mainly due to the wall compression in the direction perpendicular to the crater axis. Hence the velocity and mass of the material carried away in the primary ejection from the crater depend on the plastic and elastic characteristics of the obstacle. Of course, the probability that the background pressure in the obstacle will be superimposed on this process exists. However, for the case of collision of an individual striker with a half-infinite obstacle this can be neglected. The fourth stage of cratering takes place when the crater walls move backward from its axis. At the third stage, the vessel bottom appeared to be loaded in the process of reverse jet formation. Therefore, the walls move apart to increase the crater volume, and the bottom, because of the elastic forces, approaches the free surface. A secondary ejection with a small velocity is formed. Its mass will be largely determined by the character of adhesion of the residues of the introduced material of the striker and the matrix material fragments to the surface. The velocity of the second ejection depends on the mass thrown at this stage, the elastic forces, and the bottom area, and, all other things for source materials being equal, will be associated with the shape and velocity of the striker.

Interaction Conditions Determining the Type of Cratering. The typical cratering where the depth h is less than the sizes d_p of the striker is observed under the following conditions:

a) the volume cavity (vessel) has an open surface;

b) the third stage of cratering (compression of the walls) does not lead to a collapse and jet formation;

c) the fourth stage of cratering (expansion of the walls) is significant.

Anomalous cratering, where $6d_p \le h \le 10d_p$, takes place under the following conditions:

a) the volume cavity (vessel) has an open surface;

b) the third stage of cratering leads to a collapse and the formation of a direct and a reverse cumulative jet (mainly a reverse one);

c) the role of the fourth stage is limited.

Superdeep penetration ($10^2 d_p \le h \le 10^4 d_p$) is realized provided the following requirements are fulfilled:

a) the volume cavity (vessel) has no open surface;

b) the third stage of cratering leads to a collapse and the formation of a direct and a reverse cumulative jet (mainly a direct one);

c) the role of the fourth stage is limited;

d) in the obstacle, there is a background pressure P_b and the material strength in the crater region σ_m is small ($\sigma_m < P_b$);

e) the lifetime of the background pressure τ_b is equal to or larger than the crater (channel) formation time τ_c ($\tau_b \ge \tau_c$).

As a result of the severe deformation and superposition on it of vibrational loads in the process of cratering, the crater material along the vessel walls and bottom is in the destructured state and is likely to possess no static strength [10]. Proceeding from this suggestion, for the typical cratering to become anomalous, the following conditions should be met:

a) the depth of penetration into the obstacle $h > d_p$;

b) at the third stage of cratering, σ_m is less than the wall compression (elastic aftereffect) pressure P_e;

c) the compression (elastic aftereffect) time τ_e should be larger than the time of realization of the third stage τ_{III}.

Analysis of the experimental conditions for obtaining anomalous cratering reveals different variants of fulfilling these conditions.

The use of single microstrikers [6–8] leads to a decrease in τ_{III}. In the case where a flux of strikers is used [9, 11–13], in the obstacle a background pressure arises to provide the fulfillment of the condition $\tau_e > \tau_{III}$.

For the anomalous cratering to change to a superdeep penetration it is necessary to (a) close the open surface and (b) provide the ratio $P_b > \sigma_m$ at $\tau_b \ge \tau_c$.

In explosion welding, the conditions for typical cratering are realized. The availability of the results of this analysis of the conditions for the realization of different types of cratering at early stages of investigation (1974) made it possible to determine, at the Scientific-Research Institute of Pulsed Processes of the Belarusian State Scientific-Production Powder Metallurgy concern, the region of stable realization of superdeep penetration [1, 2, 14–16].

In bombarding the material being treated by a flux of powder particles in the bulk of steel, specific zones that are revealed due to the difference in etchability between them and the main material of the barrier arise [2]. These zones contain channel structures formed by microparticles in piercing a metal barrier. Channels ending in crater cavities with striker residues were registered. These microcavities are located at relative depths of 10^2–10^4 gauges and the ejection of the striker material from them is blocked. When metals are used as strikers, in their residues the introduced and matrix materials are revealed. When the strikers were inhibited, in the barrier metal subgauge effects, where the central rod of the striker kept piercing, throwing off the outer shell, were observed. The mass loss of the striker has a periodic character, which is likely to point to its movement with a variable velocity under the conditions of the superposition of a variable field of pressures.

The distribution of microchannels over the cross section of the obstacle is nonuniform. The highest density of channel formations is observed, as a rule, in the central part of the obstacle. For instance, in a series of investigations carried out in bombarding steel obstacles with bodies, estimation was made by means of neutron activation analysis [16], and a spread of the introduced boron distribution in the bulk of an iron obstacle is shown.

From the consideration of the features of the channel-crater formation under superdeep penetration it became obvious that the specificity of cratering in this case is in the character of the energy redistribution of the flux (bunch) impact energy on the obstacle into the channel zone.

Phenomenological Model. As we see it, of greatest interest is the approach formulated for the first time by R. Pond and K. Glass [14], which is based on the specific features of the behavior of a metal under the conditions of cratering.

The following propositions were advanced:

1. The metal behaves as if there were a time delay in cold hardening exceeding the time needed for the formation of a crater.

2. The material in the crater region does not follow the hydrodynamic laws, since the flow is only determined by the crystallographic and strength properties. The flow occurs without hardening, and once it is started, it will go on until the energy in the metal drops below a certain level.

3. The time of the process is determined by the "critical velocity" of the target metal flow.

4. As soon as the rate of motion of the material exceeds the critical velocity, large expenditures of energy for material deformation are no longer needed.

In the case of a metal (iron) obstacle, the factors providing such effects at a given scale level of interaction are the heating of the target material and the phase transitions.

Heating can be caused by the heat transfer from a particle heated in the acceleration process. However, the considerable penetration depth ($h > 10^2 d_p$), the relatively low velocities of penetration ($v_p = 300$ m/sec), and the limited heat-conductivity coefficient do not allow through penetration.

Consequently, the factor providing the possibility of decreasing stepwise the resistance to the penetration and avoiding cold hardening of the material is the phase transition inhibited at the stage of loss of long links. The proceeding of the phase transition under dynamic loading is known [17]. The following three possibilities were noted:

1) under the action of a shock wave the material goes to a denser phase (a "bend" appears on the Hugoniot curve);

2) the phase transition is accompanied by an increase in the volume (no anomalies are observed on the Hugoniot curve);

3) the phase transition is not accompanied by any noticeable change in the volume and cannot be revealed directly in shock-wave experiments.

On the basis of the foregoing a basic assumption was made in [18]. The process of superdeep penetration of the microstriker into the barrier proceeds in zones where, due to the superposition of the pressure fields, conditions sufficient for the phase transition to occur are formed. In 1983, such an assumption made on the basis of the literature data would have been more than controversial, since it required recognition of the possibility of practical realization of the superplasticity effect in microzones.

It should be agreed that during the phase transition a new state of the substance is formed [19]. The main feature of this state is the deformation inhibiting the completion of transformation and holding the substance in the state of a very high mobility unattainable under normal conditions. According to Presnyakov [19], the intermediate

state is a metastable phase in which a transformation inhibited at the stage of loss of interatomic bonds or, at least, at the stage of a sharp (by many orders of magnitude) decrease in the bonding forces develops. The appearance of the intermediate stage is explained by the fact that the intensive decay of the grid of metastable states in the process of deformation drives the body atoms to a state of enormously high mobility, which is never revealed under normal conditions. A kind of "amorphization" of the metal substance occurs. In this case, the length of the free migration of atoms turns out to be comparable to the macroscopic characteristics of the body, on the basis of which the following should be observed:

a) a high concentration of point and volume defects comparable to the defectiveness of liquid and registered in appreciable volume changes;

b) the presence of thermal effects on going to the quasi-liquid state because of the change in the bonding forces.

All these predictable effects were registered in experiments [1].

Of fundamental importance is the fact that whatever the approach declared by researchers in the narrow channel zone a decrease in the resistance to the impact penetration and energy cumulation are observed.

An example of estimation of energy cumulation in narrow zones is provided by the work of American researchers [20].

Thus, we will proceed from the following universally accepted results:

a) conditions for stable penetration of microobjects to a depth of 10^2–10^4 gauges exist;

b) the process of superdeep penetration is realized under the conditions of energy cumulation in narrow channel zones;

c) the additional energy fed into the channel zone as a result of cumulation causes the striker to move in the barrier.

Let us formulate the conditions required for the realization of the phenomenon of superdeep penetration:

a) the SDP can occur only in the case where the channel zone material is treated as a liquid and its static resistance is close to zero;

b) the impact energy of the bunch of microstrikers is cumulated in narrow channel zones.

In the most general form, the conditions enable us to state that:

a) the SDP process is self-regulating, i.e., self-similar;

b) the barrier material in long-dimensional zones with cross-section sizes not smaller than the striker diameter (d_p) decreasing with depth differs qualitatively from the source material of the obstacle.

From the assumption of incomplete phase transition in the channel zone it follows that the zone boundaries are boundaries between different phases.

Calculation of the SDP Process Energetics. We estimate the SDP energetics using the principles of minimization of assumptions and obvious underestimation of the possible values. Inhibition of the phase transition of the channel zone material is caused by the intensive deformation through vibrations of the channel walls because of the pressure gradients at the interface.

Consider the estimation of this process by an example of collision of a bunch of titanium diboride microparticles ($d_p = 40$ μm, $v_s = 745$ m/sec) with steel.

When a powder body with a mass of 0.1 kg is thrown onto a steel barrier,

$$E_s = \frac{m v_s^2}{2}. \tag{1}$$

In the SDP regime, the strikers penetrate to depths of dozens of millimeters. It is known that under macroshock loading in steel energy densities of $\sigma_{b.s} \le 1176 \cdot 10^6$ J/m^3 and in the SDP regimes $\sigma_{SDP} = 2542 \cdot 10^9$ J/m^3 are realized [21].

Under the given conditions, we estimate the penetration velocity v_p as

$$v_p = \frac{\lambda}{1+\lambda} v_s, \tag{2}$$

where $\lambda = \sqrt{\rho_s / \rho_m}$ and $v_p = 315.7$ m/sec.

We determine the number of penetrated strikers N from the experimental data on the density of channel formations ρ_c [1], assigning these values to the entire cross section of the flux S:

$$N = S\rho_c , \tag{3}$$

where $S = 1962.5\ \text{mm}^2$, $\rho_c = 200\ \text{mm}^{-2}$, and $N = 392.5\cdot10^3$ pieces.

Assume the condition for the SDP realization

$$\frac{\sigma_{b.s}}{\sigma_{SDP}} < 1 . \tag{4}$$

Then, for the SDP realization it is necessary that the energy density is increased by a factor of $2.085\cdot10^3$. The energy of single channel formation in the SDP regime is

$$E_f \geq N\sigma_{SDP}V_c . \tag{5}$$

The efficiency of using the macroimpact energy of a bunch of particles for forming the SDP channel structure

$$\eta_{en} = \frac{E_f}{E_s} . \tag{6}$$

The share of the channel structure in the obstacle

$$\eta_c = \frac{V_c N}{V_b} . \tag{7}$$

The formation time of a single SDP channel is

$$\tau_c = \frac{h}{v_p} . \tag{8}$$

For the case under consideration, $E_s = 27.75\cdot10^3$ J, $E_f = 7.241\cdot10^3$ J, $\eta_{en} = 0.2609$, $\eta_c = 153.86\cdot10^{-6}$, and $\tau_c = 30.98\cdot10^{-6}$ sec.

The kinetic energy of a single microstriker is $E_{d.e} = 11.298\cdot10^{-6}$ J.

Let us estimate the macroimpact M_{mk} and microimpact M_{pr} power of a single particle:

$$M_{mk} = \frac{E_s}{\tau_f} = 39.64\cdot10^6\ \text{W} , \quad M_{pr} = \frac{E_f}{N\tau_c} = 0.595\cdot10^3\ \text{W} . \tag{9}$$

The density of the energy obtained at the expense of the kinetic energy of a single striker can be estimated for stages I–II (b_1) and III–IV (b_2) of channeling:

$$b_1 = \frac{E_{d.e}}{V_{u.z}} , \quad b_2 = \frac{E_{d.e}}{V_c} , \tag{10}$$

where $V_{u.z} = \pi d_p^2 h/4$ and $V_c = d_{c.m}^2 h/4$.

An increase in the energy density can be attained in two ways:

1) by energy cumulation at the cost of a decrease in the channel volume $V_{u.z} >> V_c$, $V_{u.z}/V_c = 1632.5$ (experimental ratio), then $b_2/b_1 = 20{,}410$;

2) by additionally feeding the flux energy to the microstriker outside the channel:

$$\sigma_{SDP} \leq b_2 + E_{s.e} . \tag{11}$$

In the case under consideration, $E_{s.e} = 2417.6$ J/m^3, i.e., the proportion of the energy density b_2 introduced at the expense of the single striker is 1.4%. The channel compression at energy cumulation determines the striker mass loss in depth, which is observed in direct experiment [1].

Estimation of the SDP Process with Regard for the Phase-Transition Energy. Consider the case where a flux of titanium diboride TiB_2 particles is introduced into an iron obstacle. Estimate the minimum channel volume of the obstacle $V_{u.z}$ in which a phase transition is realized. From the experimental data it follows that the remainder of the striker has a size smaller than or equal to $0.05d_p$. The limiting depth from the experiment $h = 0.3$ m. We assume that the minimum channel volume of the obstacle is cone-shaped. Then

$$V_{u.z} = \frac{1}{12}\pi h d_p^2 (1 + 0.05 + 25\cdot 10^{-4}), \tag{12}$$

and in the case where $d_p = 60\cdot 10^{-6}$ m, $V_{u.z} = 2.974\cdot 10^{-10}$ m^3.

As a result of the series of experimental studies made within the framework of the Russian–Belarusian project jointly with the Institute of the Physics of Metals, Urals Branch of the Russian Academy of Sciences, it has been proved that the pressure-field distribution in the local zones of metal obstacles is essentially nonuniform and phase transitions occur in them. In particular, it is shown that on the basis of low-alloyed steels $\alpha \to \varepsilon \to \alpha$ transformations take place [22]. The high-pressure phase in them is the ε-phase. The critical pressure of the $\alpha \to \varepsilon$ transition is 12 GPa [23]. The phase ε is not retained upon removal of the load, but traces of the $\alpha \to \varepsilon \to \alpha$ cycle are seen from the changes in the microstructure. The transverse size of the zones that have undergone a cycle of transformations varies over a wide range — from fractions to 1–2 μm. It was shown that analogous structures in the Fe — 0.1% C alloy were obtained after a shock wave loading with a pressure of 20 GPa. In treating austenitic high-nickel steels, the proceeding of $\gamma \to \alpha$ with a minimum pressure of the phase transition of 8 GPa was registered. On manganese steels, $\gamma \to \varepsilon$ and $\varepsilon \to \alpha$ transformations upon treatment with a high-velocity bunch of microparticles [24] were registered.

Up to now, there has been no clear explanation of the observed effect of energy cumulation of the macroimpact energy of a bunch of microstrikers in narrow local zones of the obstacle metal. We can only think that this is a result of the superposition of the pressure fields from a train of shock waves in loading the obstacle, the unloading waves from the sample surface, and the pressure fields from the collapse and opening of the channel structures that are continuously generated and absorbed in the period of loading.

When steel containing 0.4–0.45% of carbon is used as an obstacle material, under dynamic loading, dynamic phase transitions $\alpha \to \varepsilon \to \alpha$ at a minimum pressure of $P_r = 12$ GPa, which corresponds to an energy density of $1.2\cdot 10^{10}$ J/m^3, can be realized in it. Then the energy A_f expended in the phase transition in the zone is

$$A_f = P_r V_z. \tag{13}$$

Upon etching of the defective material in the channel zone we register a visible channel pore with a mean diameter of $d_{c.m} = 0.42$. From this we obtain the volume of the channel defective zone, $V_d = 4.15\cdot 10^{-4}$ m^3.

In the vicinity of the channel the etchability of the material appreciably decreases because of the low defectiveness. Moreover, a number of research works assume that the defectiveness of the interchannel material is lower than that of the starting steel. It is logical to presume that the narrow local zone of the material that has experienced a dynamic phase transition under the action of high pulsed pressures has a raised level of defectiveness and, accordingly, of etchability. Of course, one can assume that as a result of the relaxation processes the level of defects decreases. In our opinion, however, the statement that a considerable portion of the defective material formed during the phase transitions in the narrow local zone is removed due to the ejection of a direct and a reverse jet seems more likely. Then

$$\Delta V = V_{u.z} - V_d = 297.3\cdot 10^{-12} \text{ m}^3, \quad m_c = \rho_m \Delta V = 24\cdot 10^{-6} \text{ kg},$$

where $\rho_m = 8.1\cdot 10^3$ kg/m^3.

Let us estimate the energy E_t expended in the single channel in removing this mass.

We assume that the energy introduced into the channel zone is mainly expended in ejecting the material and the channel collapse

$$A_{\mathrm{f}} = E_{\mathrm{t}} + E_{\mathrm{com}} . \tag{14}$$

Since the ejection jet is formed due to the collapse of the channel walls, we assume $v_{\mathrm{t}} = \sqrt{2}\, v_{\mathrm{com}}$. Then

$$A_{\mathrm{f}} = \frac{m_{\mathrm{c}} v_{\mathrm{com}}^2}{2} \cdot 2.414 , \quad v_{\mathrm{com}} = \sqrt{\frac{2A_{\mathrm{f}}}{m_{\mathrm{c}} \cdot 2.414}} = 1178 \ \mathrm{m/sec} , \quad v_{\mathrm{t}} = 1666 \ \mathrm{m/sec} . \tag{15}$$

The total energy in the channel zone consists of the kinetic impact energy $E_{\mathrm{d.e}}$ and the additional energy E_{m} fed from the obstacle material:

$$A_{\mathrm{f}} = E_{\mathrm{d.e}} + E_{\mathrm{m}} . \tag{16}$$

Under the assumption that $E_{\mathrm{d.e}}$ is completely expended in channeling, $E_{\mathrm{d.e}}/A_{\mathrm{f}} = 10.68 \cdot 10^{-4}\%$.

As a parameter characterizing the SDP process, we take the energy density σ_{SDP} after the passage of the striker.

To estimate σ_{SDP}, we use the approach [1]

$$E_{\mathrm{i.d}} = \int_V \int_0^{\varepsilon_{\mathrm{i}}} \sigma_{\mathrm{i}} d\varepsilon_i dv , \tag{17}$$

where $\int_0^{\varepsilon_i} \sigma_{\mathrm{i}} d\varepsilon$ is the forming energy of a unit volume.

We assume that $E_{\mathrm{i.d}} = E_{\mathrm{com}}$. It should be noted that we ignore the multistage character of channeling, including channeling at the expense of the reverse jet. We also ignore the expenditure of energy in electromagnetic radiation. Thus we obtain an obviously underestimated value of the forming energy.

We introduce the summation that the ejection Δh is formed with velocity v_{t}, and in the time of channel-wall compression — with velocity v_{com}. We determine the time of a single process τ_{s}:

$$\tau_{\mathrm{s}} = \frac{d_{\mathrm{p}} - d_{\mathrm{c}}}{v_{\mathrm{com}}} . \tag{18}$$

After a collapse the channel diameter varies in the range of 0.001–2 μm. The mean value of $d_{\mathrm{c.m}} = 0.42$ μm.

Consider three values of d_{c}. We determine the deformation from the equation

$$\varepsilon_i = \frac{\sqrt{2}}{3} \sqrt{(\varepsilon_1 - \varepsilon_2)^2 + (\varepsilon_2 - \varepsilon_3)^2 + (\varepsilon_3 - \varepsilon_1)^2} , \tag{19}$$

here

$$\varepsilon_1 = \ln\left(1 + \frac{\Delta h}{h}\right); \quad \varepsilon_2 = \varepsilon_3 = \ln\left(\frac{d_{\mathrm{p}} - d_{\mathrm{c}}}{d_{\mathrm{p}}}\right).$$

Then

$$\sigma_{\mathrm{SDP}} = \frac{4E_{\mathrm{com}}}{\theta \varepsilon_i \pi d_{\mathrm{c}}^2 h} , \tag{20}$$

where θ is the experimental coefficient equal to 1 in the first approximation. The results of the estimation are reported in Table 1.

TABLE 1. Channeling Parameters as a Function of the Finite Diameter

d_c, μm	$\tau_c \cdot 10^{-8}$, sec	$\Delta h \cdot 10^{-5}$, m	$\varepsilon_1 \cdot 10^{-5}$	$(\varepsilon_2 - \varepsilon_3) \cdot 10^{-3}$	$\varepsilon_i \cdot 10^{-4}$	σ_{SDP}, J/m^3
0.001	5.09	8.479	28.25	–0.0166	1.993	$3.547 \cdot 10^{22}$
2	4.92	8.196	27.31	–33.9	227.6	$0.776 \cdot 10^{14}$
0.42	5.05	8.413	28.03	–7.02	48.6	$8.246 \cdot 10^{15}$

From the reproducibility of experiments it follows that the SDP is stable. Obviously, conditions providing the reproducibility exist.

From the initial assumption of the dynamic phase transition in the channel zone and its incompleteness it follows that maintenance of the vibrational processes of the channel walls is realized due to the ejection of a reverse jet. O. A. Dybov [25] has proved that when a flux goes onto the rear free surface of the obstacle, direct cumulative jets piercing foils-detectors are formed on it. As the striker moves, direct and reverse jets are continuously generated in the obstacle. The probability that reverse jets move toward the frontal surface of the obstacle in the channel path is high. Therefore, while in the obstacle the process of striker penetration is proceeding, the channel zones are in the conditions of self-similar vibrations, absorbing and emitting pressure fields. The presence of the volume channel structure in the SDP process affords a self-similar system of vibrations of structural elements and stability of the process.

Determination of the Parameters of Dynamic Phase Transitions. The metal obstacle restructuring directly depends on the character of the dynamic phase transition, since it is at the expense of this process energetics that the superdeep penetration itself is realized.

From these statements the reverse assumption also follows — the parameters of the dynamic phase transition can be determined from the changes in the structure of the obstacle material subjected to treatment with a jet of microstrikers in the regime of superdeep penetration.

As the initial data, we use the experimental results [26] summarized in Table 2.

All investigations were carried out by means of threefold treatment with silicon carbide powder measuring 63–70 μm, the thrown material mass was 80 g, and the mean velocity was 700 m/sec. The obstacles were made in the form of a cylinder $5 \cdot 10^{-2}$ m in diameter and height.

From this the volume of the defective zone V_d formed in the obstacle can be determined as

$$V_d = \pi \frac{d_{c.m}^2}{4} \rho_c V , \tag{21}$$

Fe: $V_d = 0.69 \cdot 10^{-6}$ m^3, Cu: $V_d = 0.4 \cdot 10^{-6}$ m^3, and Ti: $V_d = 0.35 \cdot 10^{-6}$ m^3.

The volume of the transformation macrozone with the dynamic transition V_z is

$$V_z = \frac{E_s}{P_r} , \tag{22}$$

$$E_s = 3 \frac{m v_s^2}{2} = 5.88 \cdot 10^4 \text{ J} .$$

Since for iron it is known that in the case of the $\alpha \to \varepsilon \to \alpha$ transition $\text{Pr} = 1.2 \cdot 10^{10}$ J/m^3, we can determine $V_z = 5.0 \cdot 10^{-6}$ m^3. The SDP process under these conditions is stable and self-regulating. Therefore, we assume that

$$\frac{V_d}{V_z} \approx \text{const} = Z . \tag{23}$$

Then we estimate P_r for Ti and Cu. With the use of relation (23) we have

TABLE 2. Results of the Statistical Processing of the Structural Elements of Steel, Copper, and Titanium Specimens

Material	$d_{c.m}$, μm	ρ_c, pieces/mm^2
Steel 45	5.44	299
Copper	0.74	9048
Titanium	1.90	1217

$$\text{Ti}: \; V_z = 0.3 \cdot 10^{-5} \text{ m}^3, \quad P_r = 1.96 \cdot 10^{10} \text{ J/m}^3 \text{ (N/m}^2\text{)};$$

$$\text{Cu}: \; V_z = 0.31 \cdot 10^{-5} \text{ m}^3, \quad P_r = 1.89 \cdot 10^{10} \text{ J/m}^3 \text{ (N/m}^2\text{)}.$$

Under collisional interaction with the obstacle in the microparticle–metal matrix system three types of stress waves propagate: compression–dilatation (longitudinal) waves, shear (transverse) waves, and Rayleigh waves propagating along the surface [27]. Therefore, the boundary conditions for the realization of superdeep penetration as to the velocity can be given by the following inequality:

$$v_{cr} \le v_p \le v_{mv}. \tag{24}$$

At a collision velocity less than $v_{cr}\left(\frac{1+\lambda}{\lambda}\right)$ the pressure is lower than P_r. In the case of a collision with a velocity higher than $v_{mv}\left(\frac{1+\lambda}{\lambda}\right)$, the penetration occurs in the region of the completed phase transition, and a deformation hardening, i.e., a high value of static resistance takes place. The shear wave velocity was used as the least of the volume perturbations leading to changes in the structure in the channeling zone.

Penetration of the striker into the target in the SDP regime can only occur in the case where the striker size is equal to or smaller than the corresponding size of the region of incompleted phase transition.

The boundary condition for the striker sizes is as follows [1]:

$$K \le d_{p.m} \le C. \tag{25}$$

The size of the region C depends on the value of the pressure pulse, the background pressure in the obstacle, and the properties of the matrix material in the obstacle. It corresponds to the zone where the stresses are equal to or higher than P_r. Because the dynamic phase transition proceeds around the channel zone, an energy well arises and the energy density level increases. This is due to the fact that there is decrease in the volume of the obstacle material into which mainly the collision energy of a bunch of high-velocity microstrikers is fed. The increase in the energy due to its cumulation in the obstacle therewith turns out to be more significant than the decrease due to the reduction in the striker sizes, i.e., in the bunch density:

$$C \ge v_p \tau_{ph}. \tag{26}$$

For the case of bombarding a steel obstacle with titanium boride particles under consideration, a value of $d_{p.m} = 80$ μm was obtained by statistical processing of the experimental results [1]. On this basis

$$\tau_{ph} = \frac{d_{p.m}}{v_p} = 2.53 \cdot 10^{-7} \text{ sec}.$$

This value agrees with the data of [32].

In the case of bombarding a steel obstacle with silicon carbide particles, the obtaining of experimental values of $d_{p.m}$ is inhibited because of the silicon carbide decomposition as a result of the thermal destruction in the bunching process.

Taking into account the foregoing and making use of the difference in densities between titanium diboride and silicon carbide, we estimate the velocity of penetration of silicon carbide particles $v_p = 311.98$ m/sec. Consequently, for SiC $d_{p.m} = 78.93$ μm.

Consider the variant with a copper obstacle. We make an assumption of the possibility of phase transitions in copper in the solid state [28].

In the starting specimen we have: $V_{u.z} = V_z = V_d/Z$, $\rho = \rho_i$, $P = P_r$, $m = V_d \rho_p/Z$:

Stage I: at $\rho_1 \prec \rho_i$, $V_1 = V_z$, $P_i = P_r + \Delta P$, $m_1 = m$

$$P_r V_z = P_1 V_1 - P_1 \Delta V, \quad \Delta P = \frac{E_t}{\Delta V} = \frac{E_t}{75.92 V_d};$$

Stage II: at $\rho_2 = \rho_1$, $m_2 = m_1 - \Delta m$, $\Delta m = \Delta V \rho_i$

$$P_2 = P_3, \quad V_2 = V_z + \Delta V, \quad \Delta V = V_z - V_d;$$

Stage III: at $\rho_3 = \rho_i$, $V_3 = V_d - V_z - \Delta V$, $m_3 = m_2$

$$P_r V_z = P_3 (V_3 + \Delta V).$$

For the calculation, we used the following data: $\Delta V = 3.06 \cdot 10^{-6}$ m^3; the mass thrown from the obstacle $M_t = \Delta V \rho_i = 0.0273$ kg, $\rho_i = 8.93 \cdot 10^3$ kg/m^3, $v_{com} = 1244$ m/sec, $v_t = 1759$ m/sec, and $E_t = 4.86 \cdot 10^4$ J. Hence $\Delta P = 16.4 \cdot 10^9$ J/m^3 (N/m^2), then $m_2 = m_3 = V_d \rho_i$, $\rho_2 = \dfrac{\rho_i}{(2/Z) - 1} = 584.4$ kg/m^3.

Thus, the density in the channel zone in the second stage decreases by a factor of $\rho_i/\rho_2 = 15.28$ and recovers in the third stage owing to the decrease in the channel zone volume by a factor of $V_z/V_d = 7.69$. In the third stage thereby the density of the energy retained in the channel zone is $(A_f - E_t)/V_d = 2.6 \cdot 10^{10}$ J/m^3.

For the variant with a phase transition, with increasing density a three-stage approach is also realized. By way of example, consider iron.

In the initial stage we have: $V_{u.z} = V_z = V_d/Z$, $\rho = \rho_i$, $P = P_r$, $m = V_d \rho_i/Z$:

Stage I: at $\rho_1 \succ \rho_i$, $V_i = V_z$, $P_i = P_r - \Delta P$, $m_1 = m$

$$\Delta P_1 = \frac{E_{com}}{\Delta V} = \frac{E_{com}}{74.92 V_d};$$

Stage II: at $\rho_2 = \rho_1$, $m_2 = m_1 = m$

$$P_2 = P_r, \quad V_2 = V_z + \Delta V, \quad \Delta V = V_z - V_d;$$

Stage III: at $\rho_3 = \rho_i$, $V_3 = V_d = V_z - \Delta V$, $m_3 = m - \Delta m$, $\Delta m = \Delta V \rho_i$

$$\Delta P_3 = \frac{E_t}{\Delta V} = \frac{E_t}{75.92 V_d}.$$

For the calculation, we used the following data: $\Delta V = 4.932 \cdot 10^{-6}$ m^3; the mass thrown from the obstacle $M_t = \Delta V \rho_i = 0.038$ kg, $\rho_i = 7.83 \cdot 10^3$ kg/m^3, $v_{com} = 1118$ m/sec, $v_t = 1581$ m/sec, $E_{com} = 2.43 \cdot 10^4$ J. Hence $\Delta P_1 = 6.48 \cdot 10^6$ J/m^3 (N/m^2) in the first stage, and $P_1 = 11.99$ GPa. In the third stage, $P_3 = P_r + \Delta P_3 = 12.94$ GPa, $E_t = 4.86 \cdot 10^4$ J, $\Delta P_3 = 9.42 \cdot 10^9$ J/m^3, and $A_f/V_d = 8.64 \cdot 10^{10}$ J/m^3.

Thus, in this variant, due to the change in the sequence of stages of ejection and collapse, the energy density in the third stage is higher despite the lower pressure level of the phase transition.

Consider the experimental results of changing d_c [1]. As the channel diameter, we take the transverse size of a cavity whose etchability considerably differs from the source material of the obstacle. Such a selective etchability

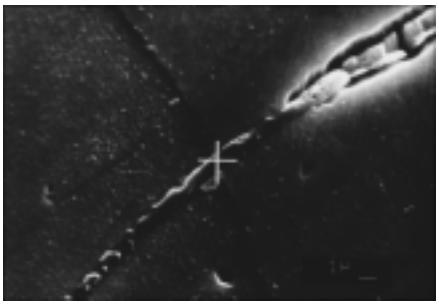

Fig. 1. Structure of the channel on the steel obstacle. ×10,000.

TABLE 3. Calculated Superdeep Channel Radius $d_c/2$ (μm) for Strikers of Different Diameters

h, mm	d_p, μm			
	5	40	50	75
0	–0.2011	0.1123	0.3246	1.772
1	0.2889	0.1914	0.3162	1.724
2	0.5161	0.2605	0.2949	1.564
3	0.5501	0.3171	0.2676	0.3074
4	0.4606	0.3584	0.241	–0.5843
5	0.3173	0.3819	0.2217	–1.28
6	0.1899	0.3849	0.2166	–1.128
7	0.1481	0.3647	0.2323	–1.1295
8	0.2615	0.3187	0.2757	+0.1939
9	0.5999	0.2444	0.3535	2.6675
10	–	0.1389	0.4724	–
11	–	0.00	0.6391	–
12	–	–0.126	–	–

can only be explained by the presence of a high defectiveness of the channel zone material. which is confirmed by the investigation of the fine structure [1]. Taking into account the realization of the fourth stage of crating, such a significant defectiveness can be explained by the high tensile stresses in this zone. It is known that depth changes in the observed diameter of the channel (d_c) have a periodic character. A typical example of such a channel on a steel metallographic section is shown in Fig. 1.

Assume that the approximation of the results by means of polynomials is legitimate. Then the obtained function $d_c = f(d_p, h)$ describes the typical character of change in the channel structure depending on the depth and the initial size of the striker. By way of illustration we show the channel diameter on a different scale. Consider the variants of the channel geometry at $d_p = 5$, 40, 50, and 75 μm. The results upon approximation for the data on d_p are given in Table 3 and the geometry of the channel zones is shown in Fig. 2.

From the results presented it is seen that depending on the initial size of the striker at different depths negative values of d_c are observed. Such negative diameters of the channels cannot be observed experimentally. However, numerous investigations of the channel structures have revealed the presence of zones without a channel cavity with a central channel rod on them (Fig. 1). The absence of selective etching away in the vicinity of the rod can only be explained by the fact that in this zone the matrix material is in the region of high residual compressive stresses. Proceeding from this, we can state that in the obstacle depth and, accordingly, in the channel depth areas of tensile and compressive stresses exist. In the former, the channel zone is etched, forming cavities on metallographic sections, and in the latter it is not etched.

This statement is additionally supported by the experimental results on the change in the density of obstacle materials upon their loading in the SDP regime [1, 29]. The series of investigations on measurement of the grid parameter of treated steel has shown that it varies in the depth of the steel obstacle [30]. This also points to the reliability of the above statement. The presence of areas of tensile and compressive stresses suggests the existence of

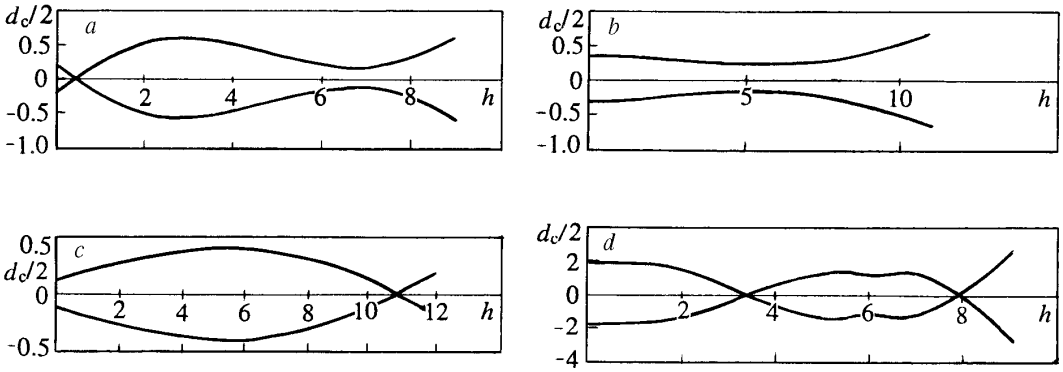

Fig. 2. Geometry of the channels obtained in the SDP regime in bombarding the steel obstacle: a) $d_p = 5$ μm; b) 40; c) 50; d) 75. $d_c/2$ μm; h, mm.

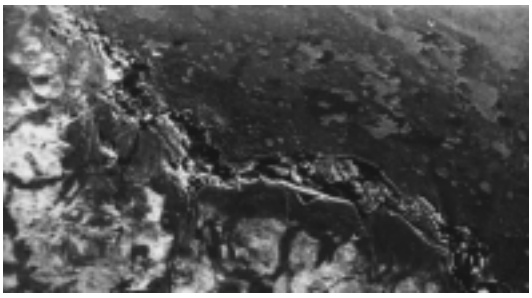

Fig. 3. Macroplate from a mixture of substances introduced in the SDP regime: tungsten, titanium, aluminum, and chrome in the subsurface layer of the steel obstacle. ×200.

interfaces between them. As a result, there is a possibility of explaining the previously established fact of inhomogeneous loss of mass of the strikers and the presence of extrema on the concentration curve of the introduced material in the obstacle depth. The existence of areas of strong compressive stresses should lead to accelerated ablation of the striker material and, accordingly, to a local increase in the concentration of the introduced substance. In limiting cases, the presence of areas of high compressive stresses can promote blocking of the SDP process.

In the case of the assumption that as a consequence of the superposition, the areas of compressive stresses of individual channel formations can form macroareas with such conditions there is a real possibility of explaining the previously described anomalous results. In particular, in determining the boundary conditions for superdeep penetration [1], the assumption of the existence of penetration limits of strikers in the SDP regime with less critical sizes was made. This was substantiated by the existence of a minimum size of the crystalline structure cell, which under the action of pulsed loading becomes unstable and destructs — undergoes a phase transition. However, the physical mechanism of such a limitation is still unclear. From Fig. 2a it follows that with a striker size less than 5 μm in the surface zone of the channel there is a region of high compressive stresses which increases in reference to the sizes of the channel zone. Apparently, if this tendency persists, then a minimum size of the striker at which in the SDP regime a region of high compressive stresses blocking penetration from the surface will be formed.

With increasing size of the striker, as the maximum critical diameter $d_{p.m}$ is approached, under the surface (Fig. 2d) a continuously increasing region of high compressive stresses arises. For the case under consideration, $d_{p.m} = 80$ μm. It is felt that at $d_p > d_{p.m}$ in the SDP regime the size of this region exceeds the size of the crater region. The cratering process is blocked and a typical crater is formed [31].

The assumption made enables us to formulate the condition for stopping the flux of particles moving in the SDP regime on a metal obstacle.

For effective deceleration of the particle flux in the obstacle, it is necessary to form at a certain depth a region of high compressive stresses having transverse sizes coinciding with the transverse size of the obstacle. With the assumption made, the sizes of this region represent a superposition of the regions formed from an individual element of the obstacle. The blocking region in the subsurface layer is realized in the case where $d_p > d_{p.m}$. We introduce into

TABLE 4. Concentration of Elements Introduced into the Obstacle

Depth h, μm	Element, mass %			
	Al	W	Ti	Cr
0	–	0.32	–	2.23
120	0.55	–	–	0.78
240	–	0.69	–	1.50
360	–	–	–	0.08
480	0.21	0.61	–	1.85
600	0.45	0.31	–	0.33
720	–	0.91	–	2.12
840	–	0.08	–	0.55
960	0.29	–	0.01	0.32
1080	0.11	0.39	–	2.82
1200	36.93	0.78	52.2	–
1320	0.21	–	–	–

the powder flow formed by an explosive accelerator ballast elements, for which we use, e.g., chrome plates of millimeter sizes.

In the real experiment, it was necessary to control the portion of the ballast element and its sizes. Since we are interested in the end result, we do not consider the whole experimental cycle in the present paper. Figure 3 illustrates the result of such an experiment.

Using microanalysis, we describe the obtained result. The obstacle material is steel 45. The content of fluctuations of Al, Cr, W, and Ti in the source material is in the range from 0.00 to 0.32 mass % for Al, from 0.00 to 0.07 mass % for W, from 0.00 to 0.38 mass % for Cr, and from 0.00 to 0.74 mass % for Ti.

Microanalysis for the presence of these elements was carried out from the surface to the plate at 120-μm intervals; the data are presented in Table 4. The concentration values were obtained after subtracting the maximum value of fluctuations. We believe that at values of 0.00 and less the concentration level is lower than or equal to the background level and put a minus in Table 4.

Table 5 gives the values of the concentrations of introduced elements without regard for the background value in the depth of the plate.

The source material elements were in the following state: aluminum – material of the metal container for the powder mixture; chrome – chrome plates (more than 3 mm in diameter) in the mixture with the powder composition; titanium, tungsten – mixture of powder particles (less than 100 μm).

The concentration of elements from the plate to the obstacle depth corresponds to the level of the source material. The results obtained show that the introduced powder materials are stopped at the boundaries of the regions of tensile and compressive stresses. The obstacle etchability before the interface and after the plate differs. The etchability of steel from the obstacle surface to the macroplate is much higher.

The introduced aluminum, which was obviously in the liquid state, doped the near-surface layer of the obstacle and the interfacial plate. The titanium was completely concentrated in the interfacial layer (plate). The tungsten was inhibited more effectively in the near-surface layer. Its concentration in the plate varies between zones from 0.03 to 96.66 mass percent. The titanium concentration in the plate varies from 0.88 to 37.5 mass percent. The concentration of aluminum varies between 0.00 and 83 mass percent.

Despite the existing notions, chromium effectively dopes the near-surface layer of the obstacle. Its concentration in this zone is firmly high and reaches a few mass percent, and in the interfacial plate it is much smaller. The result obtained for chromium can obviously be explained by the severe dynamic mass transfer. We detected no chromium inclusions in the near-layer surface. The time interval of this process of treatment for the above case remains analogous to the other variants, i.e., it is a few hundreds of microseconds. This suggests that under these conditions the dynamic mass transfer is considerably intensified.

TABLE 5. Concentration of Elements Introduced into the Plate

Depth, h, mm	Element, mass %			
	Al	W	Ti	Cr
0	31.66	7.93	26.09	0.00
5	44.43	1.77	23.21	0.78
10	25.41	22.63	28.29	0.29
15	20.69	7.85	25.08	1.59
20	26.02	2.10	14.13	0.00
25	83.67	0.95	6.41	0.00
30	36.81	3.72	9.85	0.55
35	51.56	0.00	27.82	0.06
40	35.10	0.03	37.50	0.78
45	14.46	2.89	30.01	0.93
50	0.00	96.66	0.88	2.17
55	58.40	2.83	16.74	0.53
60	37.92	10.41	18.99	0.89

The obtaining of a near-surface macroplate at depths from 1.2 to 1.5 mm is the limiting variant of blocking of the superdeep penetration of powder particles. Another limiting case will be the penetration of particles into a metal obstacle in a certain size-optimum region of collisional interactions. For the considered interaction of titanium diboride particles with steel in the region of collision with 40–60-μm strikers at depths up to 11 mm, we failed to reveal supercompression zones (zones of high compressive stresses). This apparently determines the existence of a range of conditions for optimum realization of the SDP process.

However, it should be assumed that under the same conditions for SDP, with decreasing sizes of the strikers, as a result of the penetration mass loss, at a certain depth a deviation from the optimum striker sizes occurs and zones of high compressive stresses are realized. A variant of SDP where the matrix material is involved in the penetration process is also possible. Then the striker mass increases and a deviation from the range of optimum conditions occurs. This will also lead to the formation of zones of high compressive stresses in the channel depth.

Thus, within the boundaries of the penetration conditions, in the SDP regime without the formation of zones of high compressive stresses and complete blocking of the penetration of strikers, as a result of the realization of a macroregion of high compressive stresses, "intermediate" variants should exist. The interest in them is based on the fact that in the regime of partial blocking of the penetration a complex of quite unusual conditions for acting on materials should be realized.

Let us consider this possibility. Assume that the width of the zone of high compressive stresses B is larger than $d_{\text{p.m}}$:

$$\pi d_{\text{p.m}} \geq B \geq d_{\text{p.m}} . \tag{27}$$

In this case, due to the inhibition of the introduced substance at the interface between the regions of tensile and compressive stresses an inhibition and sticking together of the strikers will occur. Then a bunch of particles — a new striker with $d_{\text{p}} \geq d_{\text{p.m}}$ — is formed.

The energy density in the zone of compressive stresses σ_{SDP1} is higher than that in the zone of tensile stresses σ_{SDP2}. If

$$\sigma_{\text{SDP1}} - \sigma_{\text{SDP2}} \geq \sigma_{\text{b.s}} , \tag{28}$$

then at the moment the bunch is inhibited due to the realization of the condition $d_{\text{p}} \geq d_{\text{p.m}}$ its capsulation will occur. In this case, the bunch of particles with sizes larger than $d_{\text{p.m}}$ will find itself in the conditions of uniform compression. The pressure of such a compression is

$$P \geq \sigma_{\text{b.s}} , \tag{29}$$

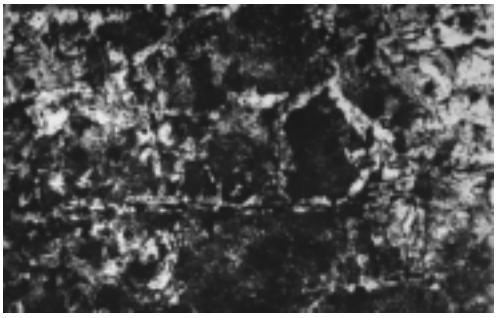

Fig. 4. Inclusion from the introduced substance in steel. ×50.

the compression time of the bunch is

$$\tau_b \geq \tau_e > \tau_{III} . \tag{30}$$

From condition (29) it follows that the material in the capsulation zone is in the plastic state and forms a globule. On the process of interaction between the introduced particles in the globule restriction (30) is imposed. As a result of the realization of the fourth stage of cratering in unloading the globule, the volume increases. Since the SDP process is accompanied by multiple loading of the obstacle material with a variable-pressure field, it may be suggested that the particles will be welded between one another, and the globule itself will in general be subjected to forging.

Consider this suggestion experimentally: we introduce changes into the previous experiment on the introduction of a mixture of Al, Ti, W, and Cr into a steel obstacle. The portion of chrome scales will not exceed 10% of the thrown substance volume, and their transverse sizes will be 3 to 4 times smaller than in the previous variant.

As a result of this variant of the SDP process, unusually large inclusions were obtained (Fig. 4). Their microanalysis has shown that they consist of W, Ti, Al, Cr, and Fe. With increasing depth of the obstacle there is a decrease in the sizes of such inclusions and a decrease in the portion of Ti and Al. The content of Cr remains approximately constant and the concentration of W and Fe increases. The shape of such inclusions becomes with depth closer to streamline [1].

Consider a typical inclusion at a depth of ~4 mm (Fig. 5). Owing to the considerable sizes of this new formation the possibility of measuring the microhardness appeared. In estimating results, the character of change in the value in different zones rather than the absolute values is important.

The treated steel had $H_\mu = 200–400$, in the vicinity of the inclusion $H_\mu = 800–1000$, and in the center of the globule $H_\mu = 1800–2000$. The obtained globules are surrounded by the matrix material. Therefore, the high temperatures in a given zone that are realized due to the intense deceleration of particles and the globule compression sharply decrease upon unloading. Hardening into a metal matrix occurs. And this permits registering an increase in the microhardeness.

The cross-section sizes of 175×108 μm of the obtained globule are shown in Fig. 5a. The prolate form obviously points to the fact that the interface between the regions of high compressive and tensile stresses is parallel to the maximum secant. Consequently, $B \geq 175$ μm. If the inclusion thickness is assumed to be equal to its width, then the globule volume will be equal to 2,041,200 μm^3.

The average particle size of Ti is 80 μm and that of W is 2 μm. In the bulk of the globule under consideration, the content of Ti ≥ 60% and of W ≤ 30%. Thus, the globule contains up to four Ti particles and up to $146 \cdot 10^3$ W particles. Apparently, the globule is a result of the consolidation of heterogeneous particles of metals.

The concentration of Fe in the globule bulk is low (Fig. 5b) and that of Ti (Fig. 5c) is high. The relatively low concentration of W (Fig. 5d) is typical of new formations at small depths. The globule structure has many deep cracks (Fig. 5a). This proves that in the SDP process this zone has been subjected to the action of intense tensile stresses. Due to the alternating loading of the globule with tensile and compressive stresses the crushing action of the process (forging in the microzones) has been realized. Because of the hardening of the metastable material of the new formation, its initial plasticity was lost and the tensile stresses have led to the cracking.

The obtaining of complex-doped materials under the conditions of dynamic loading and heat removal is a complicated technical problem. It is impossible to assess the physicochemical properties of the materials formed in the

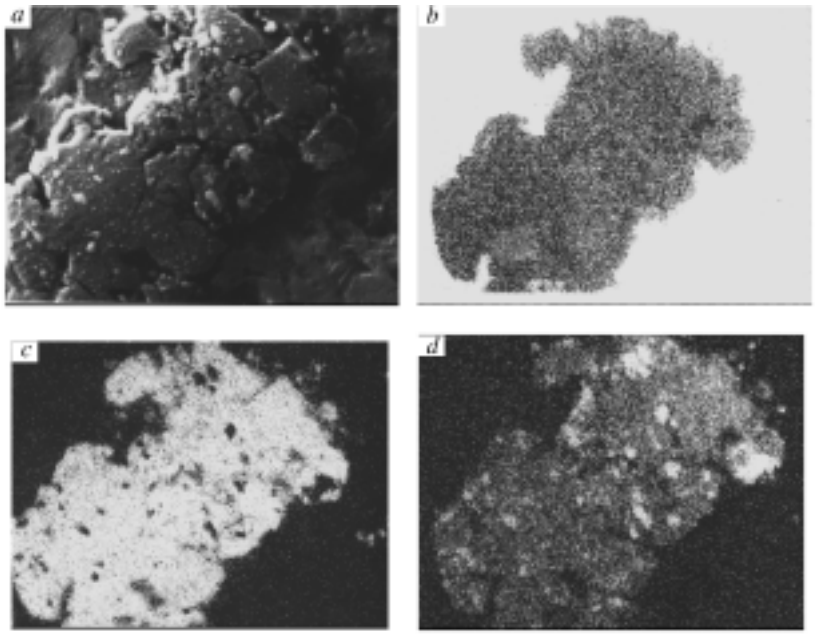

Fig. 5. Tungsten- and titanium-based globule in the steel obstacle: a) structure of the globule; b) image in the characteristic radiation on Fe; c) same on Ti; d) same on W. ×600.

globules. Therefore, the properties of the composite material arising on the basis of a metal target as a result of treatment in SDP regimes can only be assessed by means of experimental studies.

Conclusions. The consideration of the phenomenon of superdeep penetration on the basis of the set of known experimental results permits formulating a modern notion of the specificity of this process. It is based on a stable realization of the following complex of effects previously known as theoretically possible:

1) in the channel zones under the conditions of SDP, a dynamic phase transition inhibited as a result of severe deformation at the stage of loss of long links is made;

2) energy cumulation occurs due to the superposition of the pressure fields and the formation of narrow regions with a pressure level sufficient for the phase transition;

3) the process of superdeep penetration into the obstacle occurs in the zones of an incompleted phase transition with a static resistance to the striker movement close to zero, and dynamic losses are compensated owing to the feeding of energy from the obstacle material surrounding the channel region;

4) stability of the SDP process is maintained owing to the redistribution of the energy cumulated in the channel zone which is expended in the formation of direct and reverse jets and, accordingly, vibrations of the channel walls in the period of striker movement in the obstacle;

5) taking into account the simultaneous existence of the reinforcing system of channel formations (hundreds of pieces in a square millimeter during hundreds of microseconds), a self-similar vibration process in the striker flux–obstacle material system with pressure field (energy) absorption and emission is realized, and the channel zone material thereby is in the superplastic state;

6) on the basis of the initial assumption, for the first time the collapse rate of the channel after the passage of the striker and the true energy density have been estimated;

7) all kinds of cratering are determined by the conditions for the interaction of bodies, and the transition from one kind to another is caused by the introduction or exclusion of additional conditions;

8) an additional condition for the realization of penetration in the SDP regime has been formulated: the energy density realized in this regime should always be higher than at any macroimpact: $\sigma_{b.s}/\sigma_{SDP} < 1$;

9) on the basis of the analysis of the experimental data on the SDP process, the assumption that in the obstacle material macrozones of tensile and compressive stresses are formed and the boundary dimensional penetration conditions depend on the level and location of the region of compressive stresses has been formulated and substantiated;

10) in analyzing, it is necessary to take into account that the changes in the structure, etchability, density, and parameters of the crystal lattice registered by us do not reflect the real values of the stresses but are a result of the relaxation process, and the values of the stresses in the obstacle under the real conditions for the SDP process are a few orders of magnitude higher;

11) the use of the notions about the existence of macrovolumes of a material with a different type of stressed state in an individual body permits us to determine the possibilities of inhibiting the substance introduced in the SDP regime, which could not be done earlier without changing the duration of the SDP process itself;

12) additional boundary conditions for the SDP process are shown and the features of the "intermediate" regimes leading to the formation of globules whose material is a result of the consolidation of a bunch of introduced particles have been revealed;

13) on the basis of the "intermediate" SDP regimes the possibilities of developing metastable complex-doped materials under the conditions of high pulsed loadings and hardening into a metal matrix are shown.

Apparently, the SDP process under consideration makes it possible to firmly realize in microvolumes conditions previously thought to be improbable.

This work was supported by the Russian Basic Research Foundation (00–02–81017 Bel 2000) and the Belarusian Republic Basic Research Foundation (F 99P–195).

NOTATION

h, penetration depth; d_p, initial striker diameter; P_b, background pressure; σ_m, material strength in the crater region; τ_b, background-pressure lifetime; τ_c, cratering time; P_e, compression (elastic aftereffect) pressure; τ_e, elastic aftereffect time; τ_{III}, time of realization of stage III of cratering; v_p, striker penetration velocity; v_s, velocity of particle bunch collision with the obstacle; m, mass of thrown substance; $\sigma_{b.s}$, energy density under macroimpact loading; σ_{SDP}, energy density under dynamic loading in the regime of superdeep penetration; ρ_s, density of the striker material; ρ_m, density of the obstacle material; ρ_c, density of channel formations; S, flux cross section; N, number of channel formations in the cross section of the obstacle in the direction of the flux; E_f, energy of the formation of a single channel in the SDP regime; V_c, (experimental) volume of a single channel; η_{en}, efficiency of using the macroimpact energy of the particle bunch; E_s, microparticle bunch energy; η_c, share of the channel structure; V_m, volume of an obstacle with a diameter equal to the flux diameter; $E_{d.e}$, kinetic energy of the microstriker; M_{mk}, macroimpact power of the bunch; M_{pr}, microimpact power of particles; b_1, energy density under a single microimpact at cratering stages I–II; b_2, energy density at a single microimpact of cratering stages II–III; $V_{u.z}$, volume of the initial single channel zone; $d_{c.m}$, mean diameter of the channel after the action; $E_{s.e}$, specific energy fed from the obstacle material; P_r, pressure of the phase transition; α, alpha-phase; ε, epsilon-phase; A_f, energy of the dynamic phase transition in $V_{u.z}$; E_t, energy in the channel zone expended in ejecting the material; E_{com}, energy in the channel zone expended in compressing the walls; m_c, mass ejected from the channel; v_t, ejection velocity of the material from the channel; v_{com}, compression velocity of the channel walls; E_m, additional energy fed from the obstacle material; V_d, volume of the defective zone; V_z, volume of the initial channel zones of the phase-transition; ν_{cr}, critical penetration velocity; v_{mv}, rate of shear of the (transverse) wave; $E_{i.d}$, value of the strain intensity; K, size of the elementary crystal cell; C, size of the (amorphized) region of the incompleted base transition; τ_{ph}, phase-transition time; M_t, substance mass ejected from the obstacle; $d_{p.m}$, maximum diameter of the striker in the SDP regime; σ_i, stress intensity; d_c, channel diameter after the action. Dimensional quantities are given in the SI system. Subscripts: p, penetration; b, background; m, material; c, channel; e, elastic; s, impact; b.s., macroimpact; SDP, superdeep penetration; f, formation; en, energy; d.e, kinetic energy; mk, microimpact; pr, particle; u.z., unit zone; c.m, medium channel; s.e, special energy; r, reorganization; t, exchange; com, compression; d, defect; z, zone; cr, critical; mv, movement; i.d, deformation intensity; ph, phase; p.m, maximum penetration; i, intensity.

REFERENCES

1. S. M. Usherenko, *Superdeep Penetration of Particles into Obstacles and Manufacture of Composite Materials* [in Russian], Minsk (1998).

2. V. G. Gorobtsov, V. Ya. Furs, and S. M. Usherenko, in: *Powder Metallurgy*, Collection of Papers [in Russian], Issue 3, Minsk (1979), pp. 8–12.
3. S. S. Grigoryan, *Dokl. Akad. Nauk SSSR*, **292**, No. 6, 1319–1322 (1987).
4. V. P. Makarov, in: *Collection of Papers presented at IX Symp. on Combustion and Explosion* [in Russian], Vol. 1, Pt. 2, Chernogolovka (1996), pp. 331–332.
5. C. Knowls and G. Bowd, *Shock, Explosion, Destruction* [Russian translation], Moscow (1981).
6. A. T. Bazilevskii and B. A. Ivanov, in: V. N. Nikolaevskii (ed.), *Mechanics of Cratering under Impact and Explosion*, Collection of Papers [in Russian], Moscow (1977), pp. 172–227.
7. V. M. Titov, Yu. M. Fadeenko, and G. A. Shvetsov, *Dokl. Akad. Nauk SSSR*, **191**, No. 2, 298–300 (1970).
8. K. Nagel, G. Neukum, G. Eichkorn, H. Fechtig, et al., in: *Lunar Science VI*, Lunar Science Inst., Houston, Texas (1975), pp. 590–592.
9. D. Stoffter, D. Gault, I. Wedekind, and G. Polkowski, *J. Geophys. Res.*, **80**, No. 29, 4062–4077 (1975).
10. L. V. Leont'ev, *Kosmich. Issled.*, **14**, Issue 2, 278–286 (1976).
11. D. F. Wedder and J. C. Mandelvil, in: V. N. Nikolaevskii (ed.), *Mechanics of Cratering under Impact and Explosion*, Collection of Papers [in Russian], Moscow (1977), pp. 7–32.
12. M. M. Rusakov, *Prikl. Mekh. Tekh. Fiz.*, No. 4, 167–169 (1966).
13. R. E. Gannor, T. S. Laszlo, C. H. Leigh, and S. J. Wolnik, *Raketn. Tekh. Kosmonavt.*, **3**, No. 11, 148–157 (1965).
14. R. Pond and C. Glass, in: *High-Speed Shock Phenomena* [Russian translation], Ch. 8, Moscow (1973), pp. 428–467.
15. L. O. Zvorykin and S. M. Usherenko, *Metallofizika*, **15**, No. 1, 92–95 (1993).
16. S. K. Andilevko, O. V. Roman, V. A. Shilkin, and S. M. Usherenko, *J. de Physique IV, Colloque C8, Suppl. au J. de Physique III*, **4**, C8-803–C8-807 (1994).
17. A. A. Deribas, in: *Physics of Hardening and Explosion Welding* [in Russian], Novosibirsk (1980), pp. 41–111.
18. S. M. Usherenko, *Conditions for Superdeep Penetration and Development of the Process of Tool Steel Hardening by a High-Speed Flux of Powder Materials*, Dissertation for the title of Candidate of Technical Sciences, Minsk (1983).
19. A. A. Presnyakov in: *Superplasticity of Metals and Alloys* [in Russian], Alma-Ata (1969), p. 197.
20. R. D. Vound, D. L. Littlefield, and V. Horic, *Proc. AJP Conf.*, **309**, No. 1, 1821–1824 (1994).
21. S. M. Usherenko, M. Meyers, J. Owsik, and A. Zazwalska, *Fundamental Issues and Application of Shock-Wave and High-Strain-Rate Phenomena*, Albuquerque, USA (2000).
22. V. I. Zeldovich, N. Yu. Frolova, I. V. Khomskaya, et al., *Fiz. Metal. Metalloved.*, **91**, No. 6, 72–79 (2001).
23. C. H. Fowler, F. S. Minshall, and E. G. Zukas, in: *Response of Metals to High Velocity Deformation*, Interscience, New York–London (1960), pp. 275–308.
24. L. G. Korshunov, S. M. Usherenko, O. A. Dybov, and N. L. Chernenko, *Fiz. Metal. Metalloved.*, **91**, No. 6, 80–85 (2001).
25. O. A. Dybov, in: *Dynamic Restructuring of Materials* [in Russian], Ch. 1, Minsk (2000), pp. 5–21.
26. S. M. Usherenko, O. I. Koval', L. G. Korshunov, and V. I. Zel'dovich, in: *Dynamic Restructuring of Materials* [in Russian], Ch. 2, Minsk (2000), pp. 22–46.
27. Yu. A. Kharlamov and M. Kh. Shorshorov, *Fiz. Khim. Obrab. Mater.*, No. 3, 67–68 (1977).
28. H. Warlimont and L. Delaey, *Martensitic Transformations in Copper-, Silver-, and Gold-Based Alloys* [Russian translation], Moscow (1980).
29. S. K. Andilevko, E. A. Doroshkevich, S. S. Karpenko, S. M. Usherenko, and V. A. Shilkin, *Inzh.-Fiz. Zh.*, **71**, No. 3, 394–398 (1998).
30. S. M. Usherenko, G. P. Okatova, and O. A. Dybov, in: *Proc. Int. Conf. "Shock Waves in Condensed Media"* [in Russian], St. Petersburg (2000), pp. 181–182.
31. S. M. Usherenko, V. I. Gushchin, and O. A. Dybov, in: *Proc. Int. Conf. "Shock Waves in Condensed Media"* [in Russian], St. Petersburg (2000), pp. 179–180.
32. D. Bancroft, E. Peterson, and S. Minshall, *Appl. Phys.*, **27**, No. 3, 291–298 (1956).